Development of accurate contour residual stress measurement technique for sustainable structural integrity assessment in additive manufacturing

Journal of Physics: Conference Series **2811** (2024) 012033 doi:10.1088/1742-6596/2811/1/012033

Development of accurate contour residual stress measurement technique for sustainable structural integrity assessment in additive manufacturing

Mohammad Sayeed Hossain[1, 4], Tariq Al Harthy[1], Nida Naveed[2] and Carlos Garza[3]

[1] Department of Aeronautical Engineering, Military Technological College, Muscat, Oman
[2] Faculty of Technology, School of Engineering, University of Sunderland, United Kingdom
[3] Centro de Investigación e Innovación en Ingeniería Aeronáutica (UANL) Apodaca México

Abstract. Accurate analysis of residual stress present within an engineering component plays a fundamental role to its sustainable structural integrity assessment. This is particularly important for a safety critical component within the power generation sectors, aerospace, and oil and gas industries. The accurate stress analysis not only allows operators to determine the life remaining in a component but also avoid over-conservative estimates and thereby contribute to life extension of engineering plants and components. By utilizing and unifying multiple residual stress analysis tools of different nature a robust and more accurate method of stress analysis is achieved. The main aim of the current study focusses on the development and optimization of a robust residual stress tool based on the contour technique to accurately analyse inherent stress in an engineering component.

1. Introduction

Worldwide there is a year-on-year increase in consumption of energy, whilst at the same time there is increasing pressure to reduce carbon emissions. Reduction of carbon footprint is also a key concern within air travel. By specialized thermal treatment of aerospace grade aluminum alloys they are strengthened so that various aerospace parts can be manufactured using thinner section resulting in weight reduction in aircraft construction with reduced fuel consumption and carbon footprint. Thermal treatment of aluminum alloys, however, results in residual stress generation which is a major contributor to part distortion during the manufacture of aerospace components [1]. Attempts to avoid or remedy distortions cost the aerospace industry tens of millions of Euros a year [2]. Considering the impact of residual stress in design of aircraft components, engineers were expected to optimize geometric profiles and fabricate lighter aircraft [2].

The benefits derived from this study are fed directly into engineering plants including power generation, petro-chemical and aerospace industries. Accurate stress analysis can aid in life extension of ageing plants and assist in understanding how residual stress affects aerospace parts distortion and investigate ways to reduce it. More recently, additive manufacturing (AM) is being used for sustainable fabrication of complex and specialized parts, especially within oil and gas industries. The

[4] Corresponding Author: Sayeed.Hossain@mtc.edu.om

AM process, which is a form of welding, gives rise to undesired residual stress resulting from thermal cycles, temperature gradients and localized plasticity. The robust residual stress analysis technique proposed will be applied to analyze the residual stress generated by the different thermal cycles within additive manufacturing processes of a specialized component and assess its quality.

2. Residual Stress Analysis

Self-balancing interior stresses which exist within a free body at constant temperature and free from exterior loads or temperature gradients are termed residual stress (RS) [3]. The term "residual stress" is commonly used as it remains from a previous manufacturing process. Residual stresses are essentially stresses trapped in a structure. Knowledge of residual stress is important to structural integrity assessment, performance, and life extension of ageing engineering components.

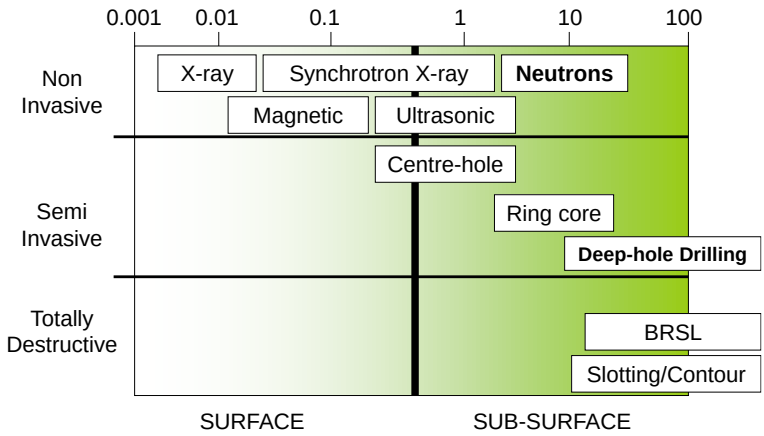

Figure 1. Classification of RS method

Several techniques [4] are available ranging from non-invasive to totally destructive, summarized in Figure 1. Diffraction, magnetic and ultrasonic (US) techniques belong to the non-invasive technique. In the application of semi-invasive methods, the part undergoes limited damage thereby maintains its integrity. Semi-invasive methods comprise incremental center hole drilling [5, 6, 7] and deep hole drilling [8, 9, 10] techniques. In a fully destructive method, the part gets completely damaged, thus compromising its integrity; techniques include Sachs technique [11, 12], layer removal method and contour technique [4, 13]. The RS methods are also classified by length scale. While X-ray diffraction (XRD) techniques [14, 15] measure near surface residual stress, the deep hole drilling and contour techniques measure RS fields deep into engineering parts.

2.1. Contour Technique

This technique is an invasive mechanical strain relief (MSR) method that gives a full uniaxial map of RS fields normal to a two-dimensional plane sectioned across the test-piece [16, 17]. The technique is built on modified Bueckner's elastic principle of superposition [18]. It involves carefully sectioning a sample into two pieces applying wire-EDM (electric-discharge machining) and measuring the resulting cut surface deformations due to redistribution of the original residual stresses. It is well-suited for spatially varying residual stress fields, with measurement size limited only by the size of the cutting machinery. The measured contour surface is examined in detail with a 0.1µm resolution surface probe. The deformations are applied as boundary condition in a finite element analysis (FEA) to reconstruct the initial residual stress field that was present within the specimen before being sectioned. As with all MSR methods the contour method endures plastic redistribution due to the sectioning of the stressed specimen [19, 20]. Much work has been carried out to mitigate the sectioning-related plasticity [21, 22, 23] by optimizing the cutting direction and the clamping strategy.

2.2. Neutron Diffraction Technique

The neutron diffraction (ND) method non-invasively measures the interior RS field in an engineering part [24, 25]. Variations in the crystals' lattice spacings, with a neutron beam incident on a part, are used to measure the strain components. There is a constructive interference, i.e., a subsequent intensity peak, when Bragg's law (Eq. 1) is satisfied.

$$2d^{hkl}sin\theta = \lambda \tag{1}$$

where d^{hkl} is the interplanar spacing between planes of Miller indices (hkl), and θ is half the angle between the diffracted and incident beams shown in Figure 2.

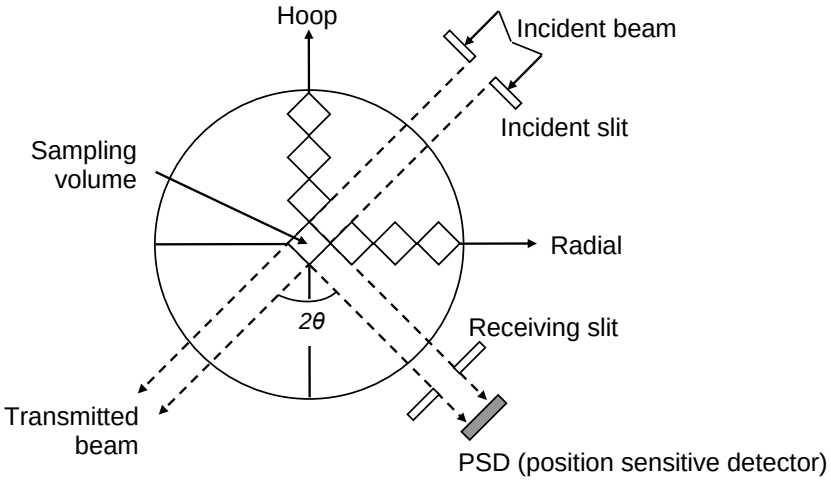

Figure 2. Schematic layout of a neutron diffractometer

A reference sample is required in the ND technique to measure the stress-free lattice spacing d_0^{hkl} which is used to determine the absolute values of residual elastic strain. Through Eq. (1) the strain component ε_i is determined in a direction defined by the geometry of the incident and diffracted beam.

$$\varepsilon_i = \frac{d_i^{hkl} - d_0^{hkl}}{d_0^{hkl}} = \frac{\Delta\lambda}{\lambda} - cot\theta\Delta\theta \tag{2}$$

The use of pulsed beam instrument ENGIN-X at Rutherford Appleton Laboratory, UK in the present study meant $\Delta\theta = 0$ in Eq. 2 and $\varepsilon_i = \Delta\lambda/\lambda = \Delta t/t$. These measured strain components through Hooke's law provide the residual stress components.

$$\sigma_{xx} = \frac{E}{(1+\nu)(1-2\nu)}\left[(1-\nu)\varepsilon_{xx} + \nu\left(\varepsilon_{yy} + \varepsilon_{zz}\right)\right] \tag{3}$$

where E is Young's modulus, and ν is Poisson's ratio of the material. Similar equations hold for yy and zz components.

3. Finite Element Analysis

Rapid spray water quenching induces a well-defined RS field within a test sample [26]. By simulating the contour technique on such water quenched specimen how the plastic redistribution of the initial as-quenched RS influences the RS field analyzed by contour method can be studied. The sample included a solid cylindrical body fabricated by type 316H stainless steel with a diameter of 60mm, and a length of 60mm, shown in Figure 3.

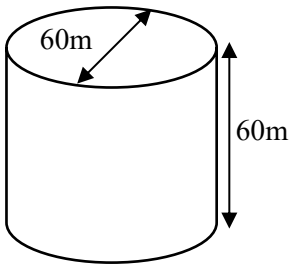

Figure 3. Schematic of the quenched cylinder.

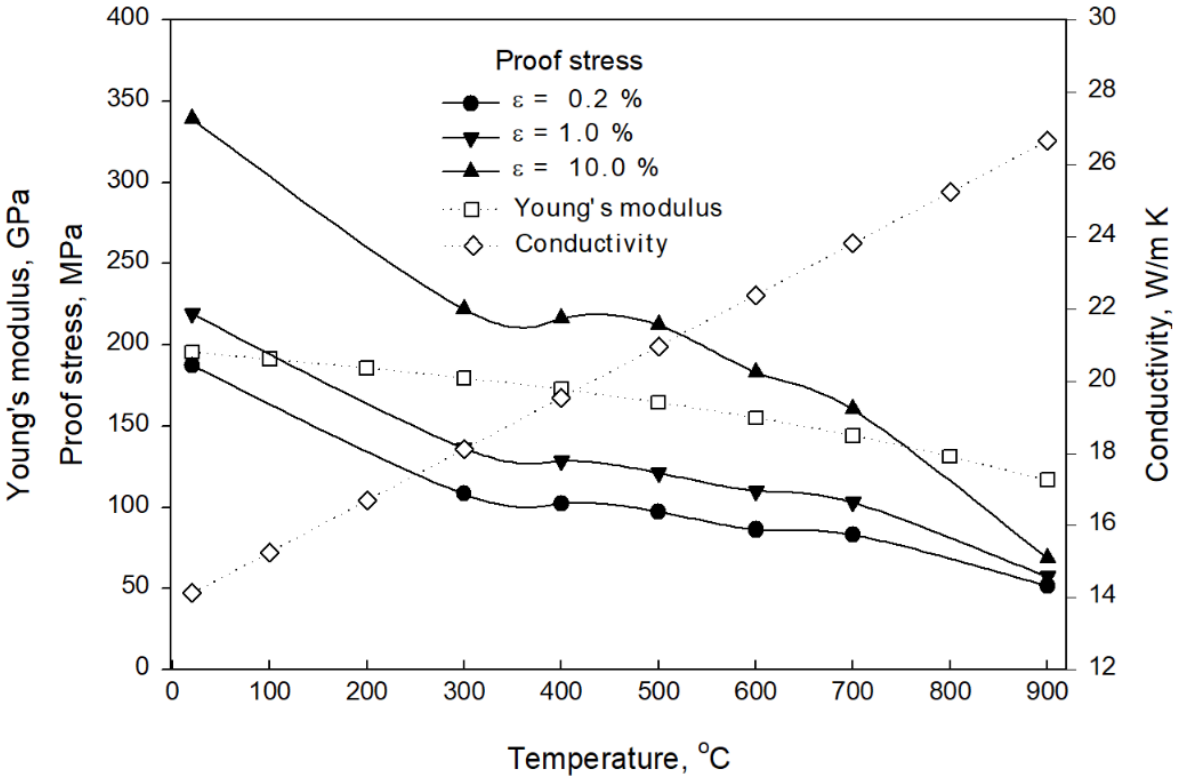

Figure 4. Type 316L stainless steel physical, mechanical and thermal properties.

3.1. Quenching Residual Stress

Residual stress in a water-quenched solid cylinder was predicted using the commercial ABAQUS version 6.12 FEA code [27]. The FEA comprised an uncoupled heat transfer with subsequent thermal stress analysis. Although quenching of the cylinder is itself axi-symmetric the subsequent model of contour method is 3D. However, due to symmetry a half model was considered. The material was assumed to be elastic with strain hardening plasticity similar to that of 316H austenitic stainless steel [28]. The material properties are temperature-dependant and are provided in Figure 4. Material properties were defined in ABAQUS input file through material data table as function of temperature [27]. The effect of phase transformation on RS and distortion was neglected for the stainless-steel material.

Thermal model: The solid cylinder was originally at constant temperature of 850°C and presumed stress-free. The outer surface was quenched in water at 20°C. Boundary conditions consisted of a convective heat transfer on the exterior surface, and adiabatic condition on symmetric planes. A thermal analysis was conducted with a uniform heat transfer coefficient 7000 $Wm^{-2}K^{-1}$ independent

of temperature. Cooling continued until the entirety of cylinder reached 20°C. ABAQUS result file stored the temperature distributions during thermal analysis. Figure 5 shows half model with contour plot of temperature distribution during cooling.

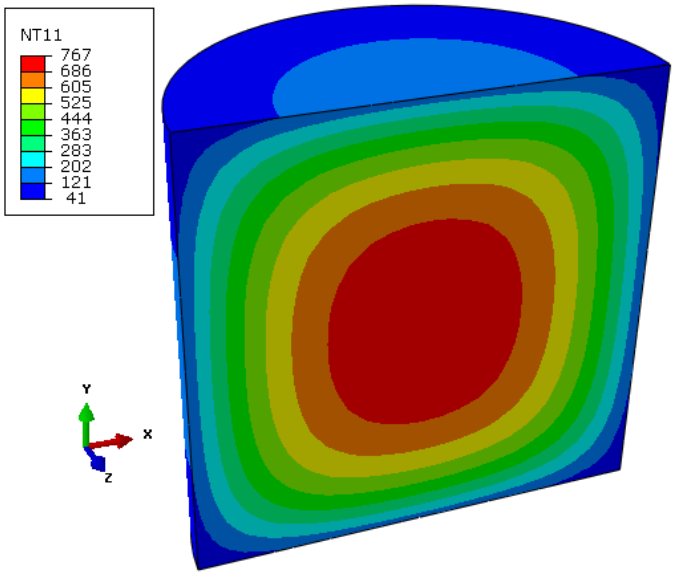

Figure 5. Half-model of the thermal model showing the temperature distribution during quenching of a solid cylinder.

Mechanical model: Temporal temperature distributions generated in each node of the thermal model was applied as input to the mechanical model. The transient stresses were substantial to produce considerable plastic flow, so that residual stresses remained after the cylinder reached the quenchant temperature. An isotropic material hardening behaviour was assumed. Figure 6 presents the x-component of the quenched RS, σ_{xx}. As expected, the inner core is in tension balanced by compression on the outer ends. Also, along x-axis the stress component on the exterior surface is zero due to free surface.

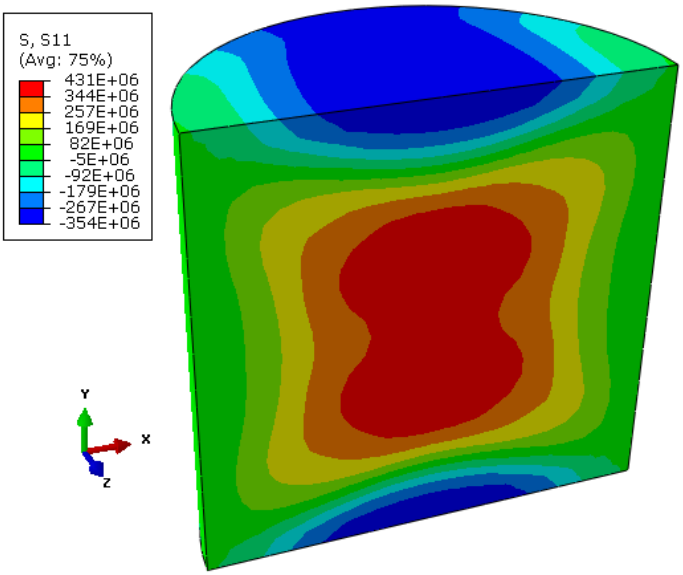

Figure 6. Half model of the mechanical model showing x-component of the quench residual stress.

3.2. Simulating Contour Technique

Contour model: The cutting (sectioning) process in the contour technique was modelled by removing a region of thickness 0.5mm, height 5mm. This was attained by utilizing the keyword "model change, remove" in ABAQUS [29]. Thus, the sectioning procedure was completed in 12 steps. Figure 7 presents the redistribution of x-component of RS on the x-y symmetry plane with the progress of cutting.

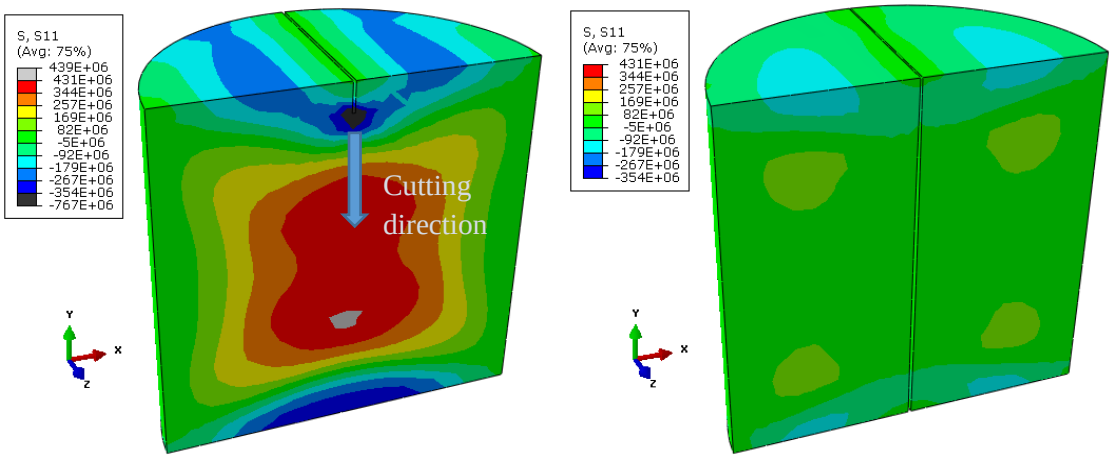

(a) Cutting Step 1 (b) Cutting Step 12

Figure 7. Contour plots showing the x-component of residual stress at the x-y symmetry plane during different stages of cutting, (a) cutting step 1, (b) cutting step 12.

4. Results and Discussions

4.1. Validation of Quenching Model

The predicted FEA temporal temperature during cooling closely correlates well with earlier measurements, see Figure 8. Figure 9 shows predicted and measured residual stress distributions across mid-section of an as-quenched 316H SS cylinder. In general, an excellent correlation can be noticed. Note that a large flight path-length (~85mm) while measuring the axial strain component at the center of the cylinder produced highly noisy data which coupled with limited count time resulted in unreliable axial strain at the cylinder center. Consequently, the ND measured RS at this position were significantly erroneous and removed from dataset. Nevertheless, since the measured residual stresses correlate well with the predicted RS about the rest of the cylinder, it is rationally assumed that a highly triaxial RS field exists near the central zone of the quenched cylinder of 20mm diameter.

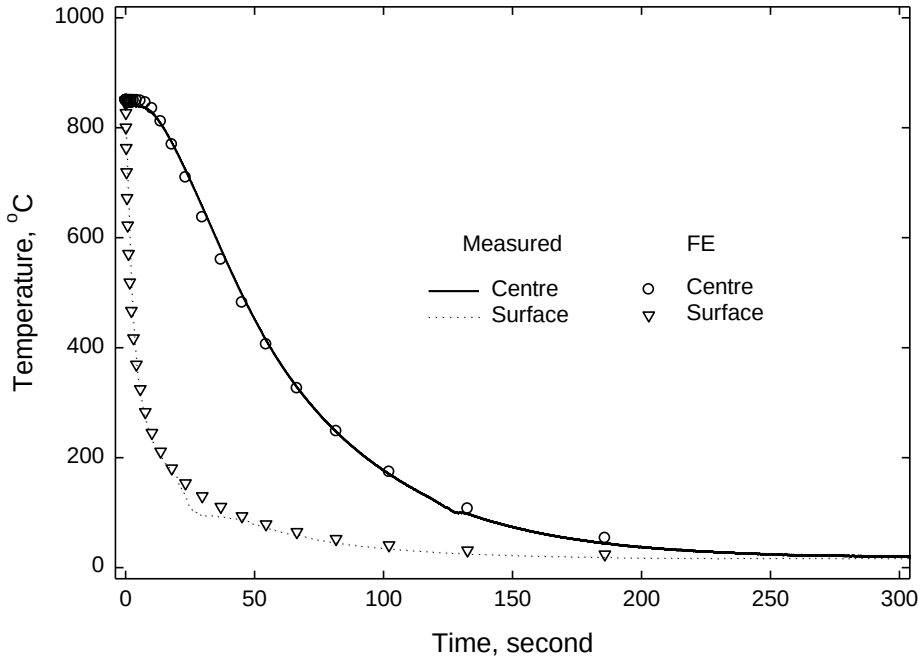

Figure 8. Temporal temperature during quenching, FEA vs measured.

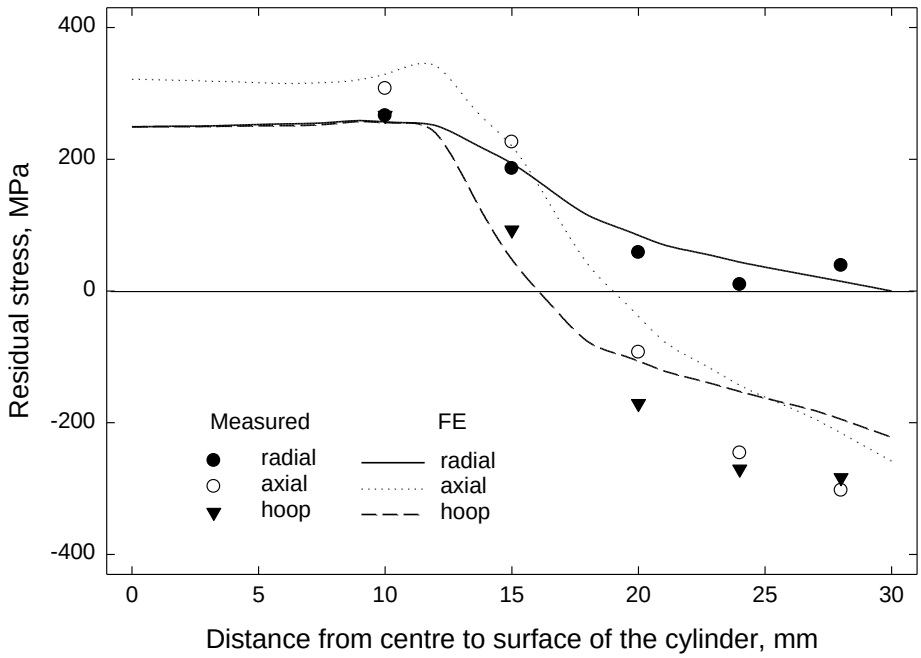

Figure 9. RS distribution across midsection of an as-quenched cylinder (diameter 60mm, length 60mm), FEA vs measured.

4.2. Reconstructed Contour Simulated Residual Stress Field

The contour method provides the stress component on the surface of the cut and normal to the surface. This surface is yz plane in Figure 7. The stress component obtained in the contour method is then σ_{xx}. Following 'cutting' process the distortions u_x perpendicular to the cut surface are obtained, see Figure 10. There are two planes (left and right sides of the cut) from which u_x components of distortions

were extracted. In practical measurements these distortions from the two surfaces are averaged in the subsequent contour residual stress reconstruction.

4.2.1. Influence of plasticity. Figure 10(a) shows the surface plot of u_x distortion under elastic-plastic analysis. The negative of these distortions were imposed on the surface of a FEA model to reconstruct residual stress fields in the contour method. Following an equilibrium step, the stress component σ_{xx} was obtained, see Figure 11. A good correlation between the contour reconstructed and the original stresses exists. However, along z axis near the free surface the reconstructed compressive stress was lower in magnitude. This is thought to be due to the presence of plasticity. To verify the influence of plasticity the analysis was repeated under elastic case. The corresponding distortion u_x under elastic analysis is shown in Figure 10(b). The effect of plasticity on reconstructed contour residual stress distribution can be seen in Figure 12.

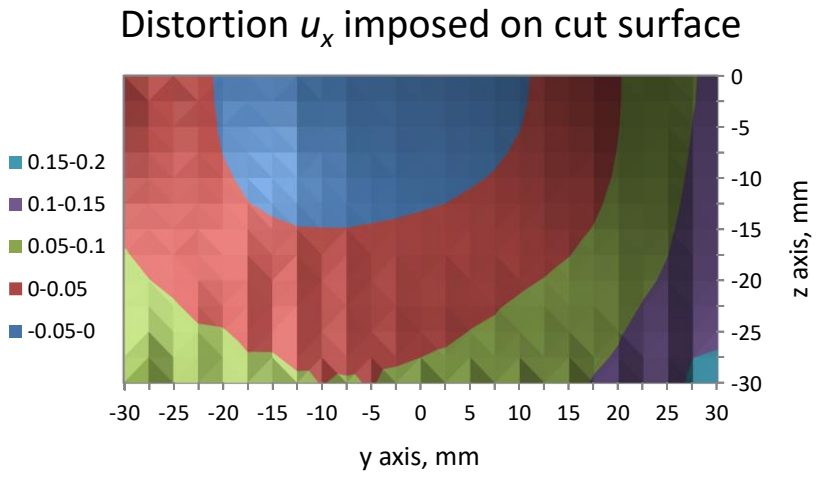

(a) Elastic-plastic Contour Analysis

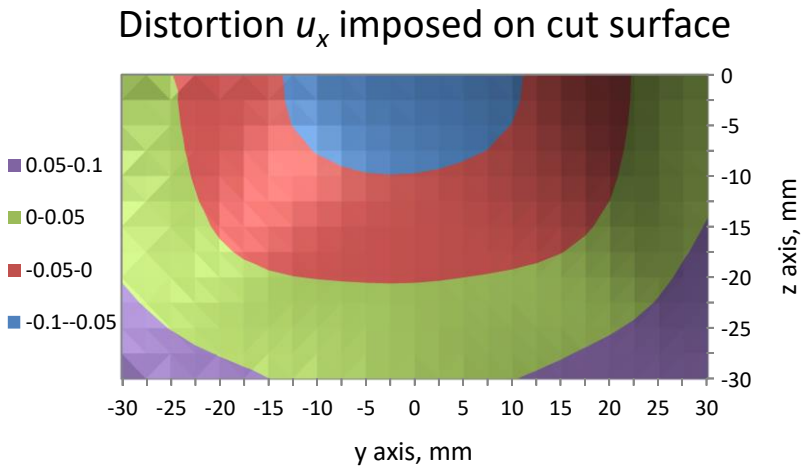

(b) Elastic Contour Analysis

Figure 10. Cut surface distortions u_x imposed on a FEA model to reconstruct contour residual stress field.

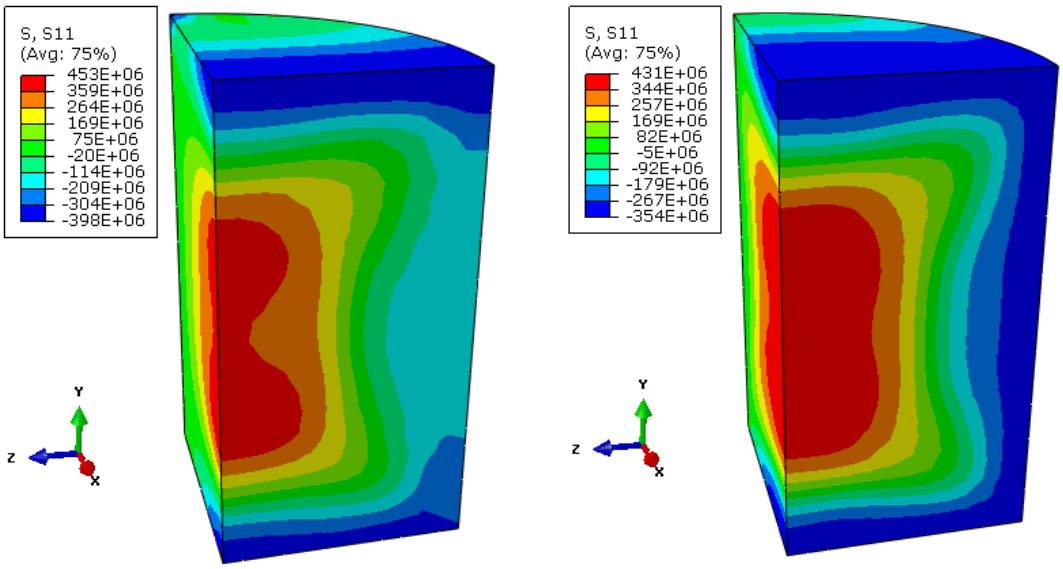

Figure 11. Comparison of (a) reconstructed residual stress x-component after imposing the u_x distortion with (b) the initial stress field.

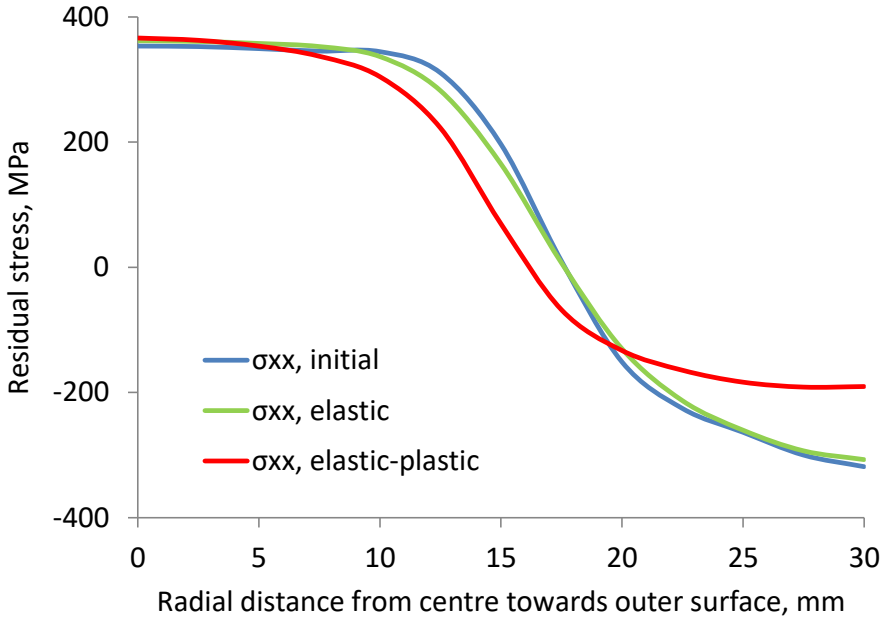

Figure 12. Comparison of reconstructed with initial σ_{xx} stress components for elastic and elastic-plastic case.

4.2.2. Influence of cutting dimension. The contour technique simulation was repeated using a reduced EDM cutting diameter of 0.1mm under elastic-plastic analysis. The results in Figure 13 clearly shows that there was no influence of the cutting dimension on the reconstructed stresses. There were no improvements by reducing the cutting diameter.

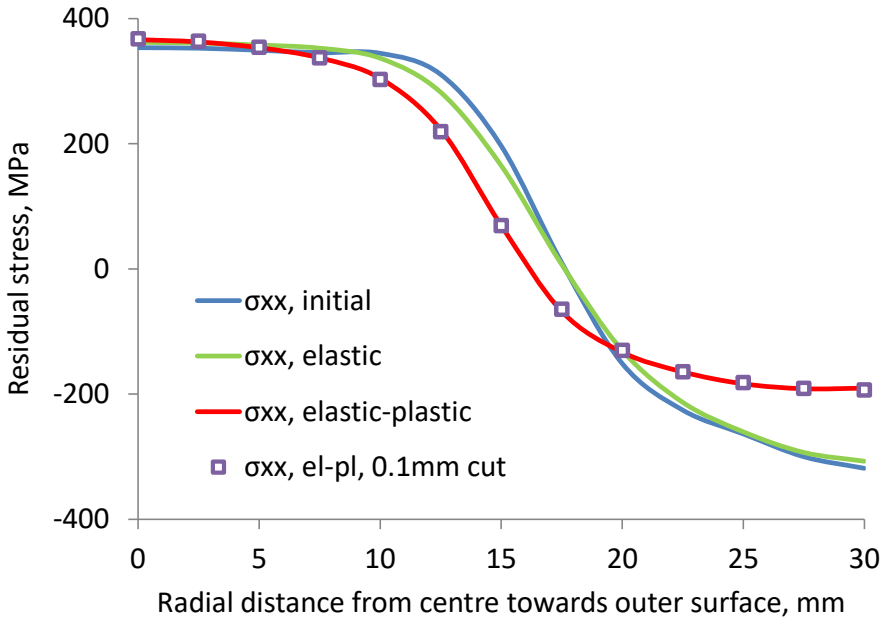

Figure 13. Comparison of reconstructed with initial σ_{yy} stress components for elastic and elastic-plastic case and using 0.1mm edm cutting.

4.2.3. Influence of cutting direction. The contour technique simulation was further repeated with different cutting direction. This is shown in Figure 14(a) where the cutting was carried out in radial direction again in 12 steps. The distortions u_z normal to the cut surface are presented in Figure 14(b). Figure 15 provides the surface plot of u_z distortion. The negative of these distortions were imposed on the surface of FEA model to reconstruct the residual stress field. The line plot shown in Figure 16 shows a good correlation between the initial and the reconstructed σ_{zz} stress components. The noise shown is due to the influence of plasticity. To verify the influence of plasticity the analysis was repeated under elastic case. The reconstructed stress under elastic analysis compares very well with the initial stress as illustrated in the figure.

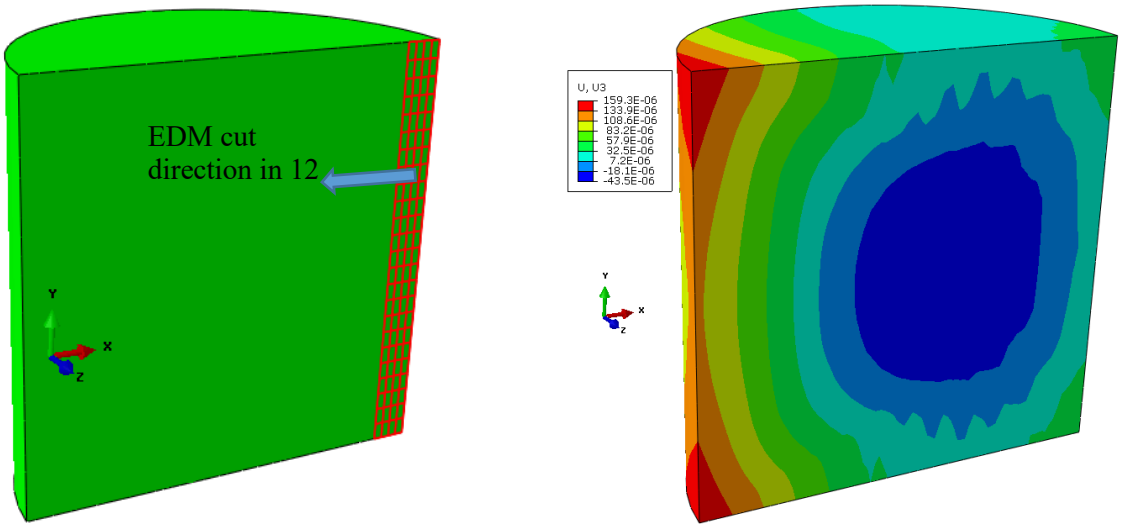

Figure 14. Contour plot showing the u_z distortion at the end of cut 12 on x-y plane for radial cut, direction shown above.

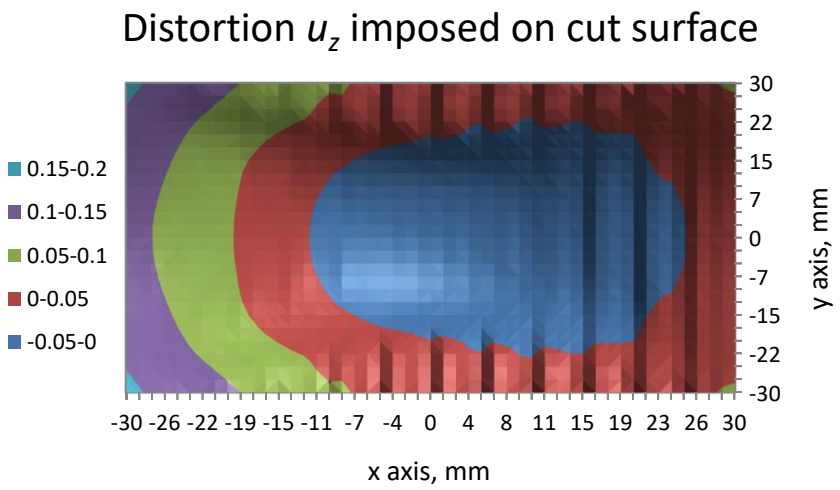

Figure 15. Distortion u_z, for radial cut at the cut surface, negative of which is imposed on the FEA model to reconstruct the contour residual stress fields.

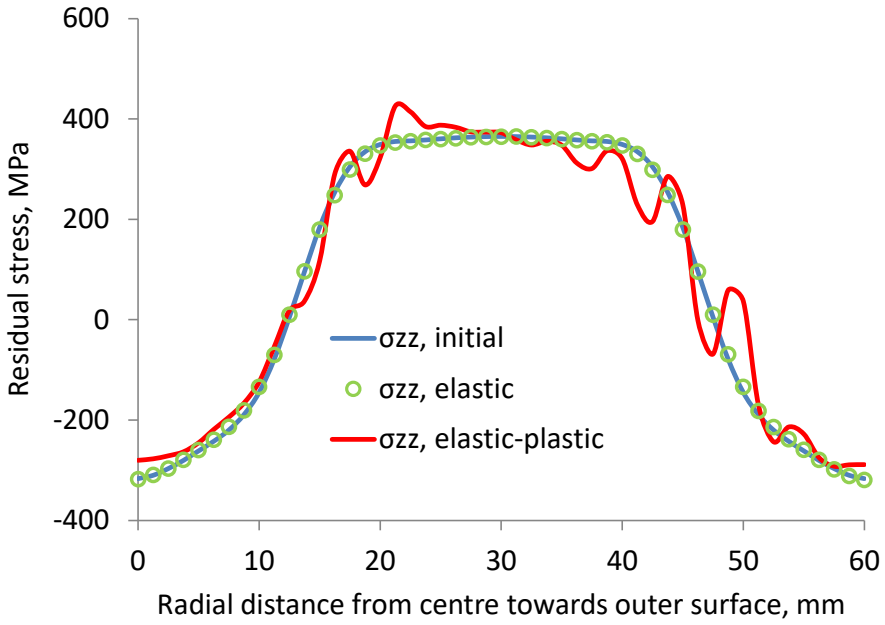

Figure 16. Comparison of reconstructed and initial σ_{zz} stress components for elastic and elastic-plastic case.

4.3. Development and optimisation of contour method

The contour method provides a contour map of RS field in an engineering component mock-up that can be used to benchmark other essential measurement techniques such as hand-held US/XRD portable device. The novelty and originality of the current research includes applying a non-contact digital image correlation (DIC) method to gage surface deformation in a sectioned surface in the contour technique. DIC has successfully been utilized in other MSR methods, e.g., hole drilling method [30, 31] but has never been applied in contour method. The application of DIC in contour method is novel and can advance the knowledge of the conventional contact based CMM technique to non-contact DIC technique.

5. Conclusions and Future Work

A knowledge of through-thickness RS distribution is vital for precise structural integrity assessment. An accurate estimate of the stress can avoid over-conservative assessment and extend the life of an engineering component. The contour technique like any MSR technique also suffers from plastic redistribution during its application. The present study showed the FEA to be a powerful tool for optimizing the strain relief RS measurement techniques.

To test and validate the development of residual stress measuring tool, benchmark samples will be carefully designed and manufactured as future work, and include:

- A well characterized residual stress in as-quenched specimen of stainless steel.
- A well characterized residual stress in as-welded stainless-steel specimen.
- A well characterized residual stress in as-quenched aluminum specimen.

Residual stresses generated within these quenched and welded samples will be modelled and predicted in FEA and measured using other techniques such as the ND technique. These results may be used to validate the DIC-assisted contour technique developed in the present study.

Acknowledgments

The authors are grateful for the financial support by the Ministry of Higher Education Research and Innovation Oman.

References

[1] Bowden DM, Sova BJ, Beisiegel AL and Halley JE 2001 Machined Component Quality Improvements Through Manufacturing Process Simulation, *SAE Technical Paper* 2001-01-2607, https://doi.org/10.4271/2001-01-2607.

[2] COMPACT 2005 A concurrent approach to manufacturing induced part distortion in aerospace components, Grant agreement ID: 516078, Funded under FP6-AEROSPACE.

[3] Withers PJ and Bhadeshia KDH 2001 Residual stress: Part 2 – nature and origins, *J. Mater. Sci. Technol.*, **17**(4), 367–375.

[4] Withers PJ and Bhadeshia KDH 2001 Residual stress: Part 1 – measurement techniques, *J. Mater. Sci. Technol.*, **17**, 355–365.

[5] Schajer GS 1998 *J Eng Mater Technol*, **110**, 338.

[6] Schajer GS 1998a *J Eng Mater Technol*, **110**, 344.

[7] Hossain S, Daymond MR, Truman CE and Smith DJ 2004 Prediction and measurement of residual stresses in quenched stainless-steel spheres, *Materials Science and Engineering A* **373**, 339-349.

[8] Zheng G, Hossain S, Kingston E, Truman CE and Smith DJ 2017 An optimisation study of the modified deep-hole drilling technique using finite element analyses applied to a stainless steel ring welded circular disc, *International Journal of Solids and Structures*, **118-119**, 146-166, https://doi.org/10.1016/j.ijsolstr.2017.04.008.

[9] Hossain S, Truman CE and Smith DJ 2012 Finite element validation of the deep hole drilling method for measuring residual stresses, *International Journal of Pressure Vessels and Piping*, **93-94**, 29-41.

[10] Kingston EJ, Stefanescu D, Mahmoudi AH, Truman CE and Smith DJ 2006 Novel applications of the deep-hole drilling technique for measuring through-thickness residual stress distributions. *J ASTM Int* **3**(4):1-12.

[11] Garcia-Granada AA, Smith, DJ and Pavier MJ 2000 A new procedure based on Sachs boring for measuring non-axisymmetric residual stresses, *International J. of Mechanical Sciences*, **42**, 1027-1047.

[12] Sachs G 1927 Nachweic innerer spannungen in stange und rohren, *Zitschrift fur Metalkunde*, **19**, 352-357.

[13] Treuting RG and Read Jr WT 1951 A Mechanical Determination of Biaxial Residu-al Stress in Sheet Materials, *Journal of Applied Physics*, **22**(2), 130-134.

[14] Sedighi M and McMahon C A 2000 The influence of quenchant agitation on the heat transfer

coefficient and residual stress development in the quenching of steels, *Proc. of the Institution of Mechanical Engineers*, *Part B: Journal of Engineering Manufacture*, **214**(7), 555–567. https://doi.org/10.1243/0954405001518251.

[15] Yazdi SR, Retraint D and Lu J 1998 Study of through-thickness residual stress by numerical and experimental techniques, *The Journal of Strain Analysis for Engineering Design* **33**(6), 449-458. https://doi.org/10.1243/0309324981513147.

[16] Prime MB 2001 Cross-sectional mapping of residual stresses by measuring the surface contour after a cut, *J. Eng. Mater. Technol.*, **123**(2), 162–168.

[17] Prime MB and DeWald AT 2013 Chapter 5 in Practical Residual Stress Measurement Methods, Gary S. Schajer, Editor, 109-138. ISBN: 978-1-118-34237-4. DOI: 10.1002/9781118402832.ch5.

[18] Bueckner H F 1958 The propagation of cracks and the energy deformation, *Trans. ASME*, 80, pp. 1225–1230.

[19] Traoré Y, Hosseinzadeh F and Bouchard PJ 2014 Plasticity in the contour method of residual stress measurement. *Advanced Materials Research*, **996**, 337-342, https://doi:10.4028/www.scientific.net/AMR.996.337.

[20] Hossain S, Zheng G and Goudar D 2020 Advances in analysis of total uncertainties in a semi-invasive residual stress measurement method. *Strain*, 2021; **57**: e12368. https://doi.org/10.1111/str.12368.

[21] Hosseinzadeh F, Traore Y, Bouchard PJ and Muránsky O 2016 Mitigating cutting-induced plasticity in the contour method. Part 1: Experimental, In*ternational Journal of Solids and Structures*, **94–95**, 2016, 247-253, ISSN 0020-7683, https://doi.org/10.1016/j.ijsolstr.2015.12.034.

[22] Sun YL, Roy MJ, Vasileiou AN, Smith MC, Francis JA and Hosseinzadeh F 2017 Evaluation of errors associated with cutting-induced plasticity in residual stress measurements using the contour method. *Experimental Mechanics* **57**, 719-734. https://doi.org/10.1007/s11340-017-0255-5.

[23] Kim HK, Carlson SS, Stanfield ML, Paddea S, Hosseinzadeh F and Bouchard PJ 2022 Mitigating Cutting-Induced Plasticity Errors in the Determination of Residual Stress at Cold Expanded Holes Using the Contour Method. *Experimental Mechanics* **62**, 3-18. https://doi.org/10.1007/s11340-021-00756-z.

[24] Fitzpatrick ME and Lodini A 2003 Analysis of residual stress by diffraction using Neutron and Synchrotron radiation. *Taylor & Francis*, London.

[25] Lewis SJ, Hossain S, Smith DJ, Truman C E and Hofmann M 2011 Determination of Remnant Residual Stresses in Fracture Toughness Specimens Extracted From Large Components, *Strain*, **47**(1), 333-343. doi: 10.1111/j.1475-1305.2009.00614.x

[26] Hossain S, Truman CE, Smith DJ and Daymond MR 2006 Application of quenching to create highly triaxial residual stresse in type 316H stainless steels, *International Journal of Mechanical Sciences*, **48**, 235-243.

[27] ABAQUS INC. 2012 *ABAQUS/standard user's manual*, 6.12 ed

[28] Hossain S, Truman CE, Smith CE and Bouchard PJ 2006a Measurement of residual stresses in a type 316H stainless steel offset repair in a pipe girth weld, *Journal of Pressure Vessel Technology*, **128**(3) 420-426, DOI: https://doi.org/10.1115/1.2218346

[29] Hossain S, Kingston E, Truman CE and Smith DJ 2011 Finite element validation of the over-coring deep-hole drilling technique, *Applied Mechanics and Materials* **70**, 291-296, doi:10.4028/www.scientific.net/AMM.70.291

[30] Chen Y, Chen X, Xu N and Yang L 2014 The digital image correlation technique applied to hole drilling Residual Stress Measurement, *SAE Technical Paper* 2014-01-0825, https://doi.org/10.4271/2014-01-0825.

[31] Gao J and Shang H 2009 Deformation Pattern Based Digital Image Correlation Method and its Application to Residual Stress Measurement. *Applied Optics*, 48(7), pp.1371-1381.